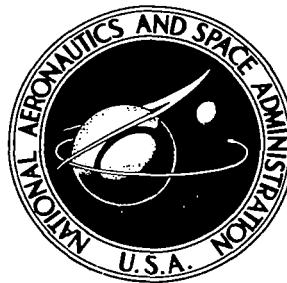


NASA TECHNICAL NOTE



NASA TN D-4634

2.1

NASA TN D-4634

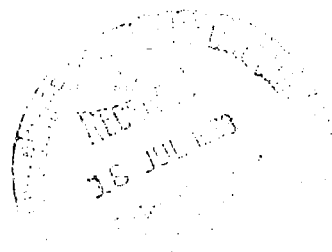


LOAN COPY: RETURN TO
AFWL (WLQ-2)
KIRTLAND AFB, N MEX

A PRECISION SPACECRAFT RADIOMETER FOR HECTOMETER WAVELENGTHS

by C. R. Somerlock and J. Krustins

*Goddard Space Flight Center
Greenbelt, Md.*





A PRECISION SPACECRAFT RADIOMETER
FOR HECTOMETER WAVELENGTHS

By C. R. Somerlock and J. Krustins

Goddard Space Flight Center
Greenbelt, Md.

NATIONAL AERONAUTICS AND SPACE ADMINISTRATION

For sale by the Clearinghouse for Federal Scientific and Technical Information
Springfield, Virginia 22151 - CFSTI price \$3.00

ABSTRACT

The Radio Astronomy Explorer program at Goddard Space Flight Center has pointed out the need for sophisticated radio astronomy receivers for spacecraft use. Development of such a receiver is described with design details. The resulting instrument is a feedback radiometer of the Ryle-Vonberg type. It measures at nine different frequencies between 0.4 Mc and 10 Mc with a 60-db dynamic range centered at an antenna temperature of 10^6 °K. The incorporation of a novel thermistor-bridge power meter yields a long-term measurement accuracy of $\pm 1/2$ db.

CONTENTS

Abstract	ii
INTRODUCTION	1
SYSTEM DESIGN	1
CIRCUIT DESIGN	4
Dicke Switch	4
RF Amplifiers	4
Oscillators	5
Mixer	5
IF Filter	5
IF Amplifier	6
Detectors	6
Phase-Sensitive Demodulator	9
Integrator	9
Noise Source	9
Range-Attenuator and Logic	10
Thermistor-Bridge	10
Reference Oscillator	12
RESULTANT HARDWARE	12
References	15

A PRECISION SPACECRAFT RADIOMETER FOR HECTOMETER WAVELENGTHS

by

C. R. Somerlock and J. Krustins

Goddard Space Flight Center

INTRODUCTION

Since the birth of radio astronomy, astronomers have tried to measure cosmic noise at the low end of the radio spectrum. Below about 10 Mc, these measurements have been severely hampered by the earth's ionosphere. These inherent difficulties of ground-based low-frequency observations have created a new, wide interest in satellite radio astronomy.

During the last few years, several radio-astronomy experiments have been flown on board space vehicles and sounding rockets and have provided interesting and controversial data. In general, all these experiments have used simple instruments and nearly omnidirectional antennas—devices whose accuracy, stability, and resolution are poor compared to those used on the ground.

Because of the need for improved scientific data, it was decided that the Radio Astronomy Explorer project at GSFC should encompass "second generation" experiments. That is to say, an attempt would be made to improve antenna directivity and measurement accuracy by an order-of-magnitude. To provide this type of data for the RAE mission, the experiment instrumentation would have to meet the following objectives:

1. Measure to an accuracy of $\pm 1/2$ db,
2. Respond to a 60-db range of signal inputs centered at 10^6 °K,
3. Measure over a decade span of input frequencies,
4. Operate for approximately 1 year in the space environment,
5. Maintain or check calibration during this 1-year lifetime, and
6. Use little power and space.

The first three objectives were readily achievable in ground-based instrumentation, but what made these specifications unique was the combination of these requirements with the needs for miniaturization and long-term unattended operation. Development work on a device to meet these objectives was begun in mid-1963 at GSFC and eventually resulted in this radiometer.

SYSTEM DESIGN

The most stringent requirement for the device was that it make stable, precise measurements unattended, in the space environment over a long time. Because of this requirement for extreme stability the basic system chosen was a feedback radiometer of the Ryle-Vonberg type (Reference 1). In this type of instrument, antenna noise is measured by constant comparison with an internal

voltage-controlled, calibrated noise source adjusted by a servo loop to equal in magnitude the unknown antenna signal. Because this unit measures by nulling, it is very insensitive to internal changes in system gain or bandwidth. Figure 1 is a basic servo-system radiometer block diagram.

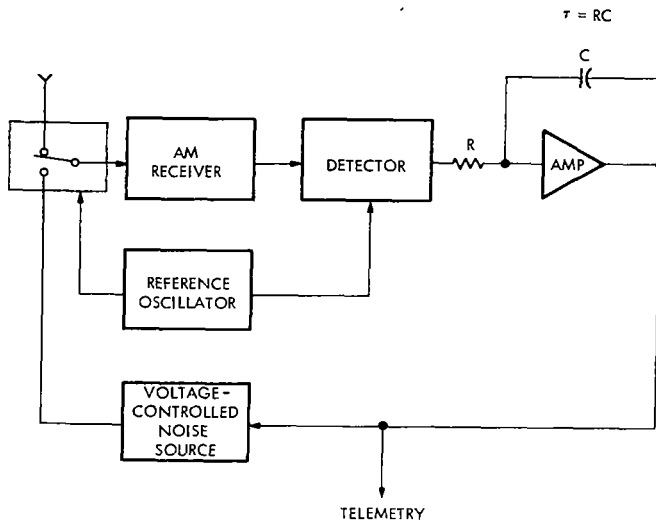


Figure 1—Basic servo system radiometer.

This technique, of course, places the entire burden of calibration on the internal voltage-controlled noise source. Thus—to insure that the measurement accuracy would be everything that was desired, and to provide some redundancy in this area—a novel addition was made to the standard Ryle-Vonberg system: a stable thermistor-bridge power meter was added to continuously measure the output power from the internal noise source. The desired antenna noise measurement is therefore made in two ways: (1) by telemetering the noise-source control voltage (coarse) and (2) by telemetering the output of the thermistor-bridge (fine). These two outputs provide redundant information, except that the bridge measurement is inherently more stable and precise. Figure 2 shows the original circuit with the thermistor-bridge and an attenuator added.

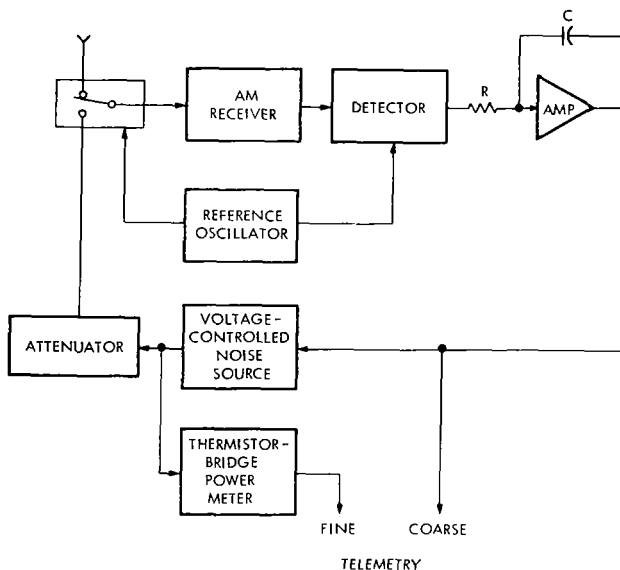


Figure 2—Addition of thermistor bridge to servo system radiometer.

The time constants of these two feedback loops were chosen as compromises between a rapid response necessary to examine dynamic phenomena and a slow response to improve antenna temperature resolution for the mapping of background radiation. Because of the ambient temperature-dependence of the coarse telemetry output, short-term measurements are more useful than long-term ones. The 0.1-second time constant of this loop emphasizes the dynamic measurements. The fine telemetry signal has a longer time constant, of about 0.5 second; this reduces the statistical noise superimposed on this output voltage and makes for more accurate long-term mapping. Although a still longer time constant could easily have been provided, an upper limit was set by antenna beamwidth and rate at which it scans the sky.

The RF bandwidth of the receiver is likewise a compromise. Great bandwidths improve sensitivity and resolution (minimum detectable signal variation), but small bandwidths are less susceptible to interference from discrete man-generated frequencies. The 40-kc bandwidth used is just under one-tenth of the lowest measurement frequency.

The resolution of a radio-astronomy receiver is normally defined as the RMS statistical noise on the receiver's detected outputs. This is considered the smallest change detectable by "eyeball integrating" the chart recording; its value depends on the instrument's bandwidth and time constant as described by the radiometer equation:

$$\frac{\Delta T}{T} \cong \frac{\sqrt{\pi/2}}{\sqrt{BW \cdot \tau}} \quad (1)$$

For this instrument, this quantity turns out to be:

$$\frac{\Delta T}{T} \cong \frac{\sqrt{\pi/2}}{\sqrt{4 \times 10^4 \times 0.5}} \cong 1 \text{ percent}.$$

However, in an application such as satellite-borne radio astronomy where the radiometer output is *sampled* at a rather low rate, peak noise might be a better resolution criterion than RMS noise level, for a single sample. Therefore, the actual resolution $\Delta T/T$, of the instrument in this application is probably about four times larger, or approximately 4 percent.

There are many ways to make measurements over a wide frequency range. Here, it was decided to use a superheterodyne receiver and incorporate separate tuned RF amplifiers and local oscillators for each desired frequency. These individual "front-ends" are turned on and off in sequence. This technique has the following advantages over a wideband input:

- fewer spurious responses,
- less probability of cross-modulation between signals, and
- redundancy.

The wide range of input frequencies can also make it hard to eliminate images. Since this device was intended to measure wideband noise, it was decided to use a very low-frequency IF and use the image as part of the intended input instead of filtering it out.

Finally, because the dynamic range of the thermistor-bridge is limited to about 20 db, a switchable attenuator was provided between the noise-source output and the Dicke-switch input at the receiver front end. With associated logic circuits, this attenuator automatically changes ranges to provide a total dynamic range of 60 db. The complete radiometer block diagram is shown in Figure 3.

CIRCUIT DESIGN

Dicke Switch

The Dicke switch (antenna switch) that alternately switches the radiometer input between the antenna and the internal noise source is basically a single-pole double-throw switch (see Figure 23).^{*} It consists of two field-effect transistors that are alternately biased on and off by out-of-phase 100-cycle square waves. These transistors provide excellent isolation between the signal path and the switching waveform, thus reducing switching transients. These transients are also reduced by the low switching frequency, which minimizes the harmonic energy from the driving square wave that falls in the frequency range of the radiometer input. For the same reason, the rise time of the 100-cycle square wave is stretched to about 1 millisecond. Because of the necessity of integrating this 100-cycle chopping frequency in the radiometer's servo-loop, the low switching frequency places a lower limit of about 0.1 second on the servo-system's time constant.

RF Amplifiers

The first RF amplifier serves two functions. It provides RF gain, and restricts the frequency spectrum of the noise entering the radiometer to a 200-kc band around the frequency of interest. A separate tuned amplifier is used for each frequency, instead of a single amplifier (with electronically switched tuning elements) for all the frequencies. This method simplifies switching and improves system reliability, since the loss of one RF stage means only the loss of that particular frequency and not the loss of the whole radiometer.

There are nine separate first RF stages. The inputs of all nine are connected together, whereas the outputs are switched with diode switches to the second RF stage. Power is applied only to the stage switched into the radiometer, thus conserving dc power. The other eight stages are not biased on and their diode switches are open; this prevents noise at the other frequencies from reaching the receiver.

The individual stages are tuned amplifiers that provide about 30-db RF gain and have about 25-db AGC capability. Their bandwidth is about 200 kc and is not critical, since the radiometer bandwidth is set by the narrower IF filter.

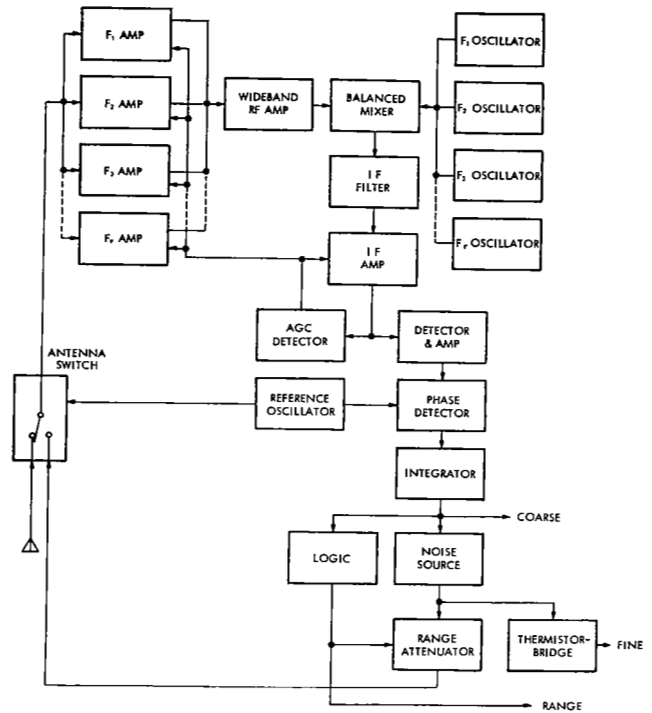


Figure 3—Radiometer block diagram.

^{*}Figure is a fold-out schematic at end of this paper.

The second RF stage is a wideband amplifier providing 10 db of additional RF gain.

Oscillators

Crystal oscillators are used so as to provide good frequency stability (Figure 23). Separate oscillators are used for each frequency for the same reasons that separate RF amplifiers were used: it simplifies switching and improves reliability. The oscillators are connected with diode switches to the mixer; bias is supplied only to the stage that is "on."

Parallel resonant crystals that require a loading capacitance of 32 pf are used. The capacitance used in the feedback network, C_4 and C_5 , must therefore be low, that is, of high reactance at lower frequencies. Because of this, a field-effect transistor was used to provide a high input impedance that does not load down the feedback network. Feedback is heavy, to insure oscillation if the transistor gain is reduced by aging or environment. The output is tuned to reduce waveform harmonic content.

Mixer

The mixer (Figure 23) converts the RF noise down to frequencies between 10 and 30 kc. The inputs to the mixer are the local oscillator and a band of noise, 200-kc wide, centered on the local-oscillator frequency. The mixer output contains the difference frequencies between the local oscillator and the RF noise input. These will range from 1 cycle to about 100 kc. The filter in the output of the mixer selects only noise in the region 10-30 kc and rejects all other frequencies. Since noise on either side of the local oscillator will give difference frequencies in the range 10-30 kc, the mixer is sensitive to two 20-kc segments, thus providing a total 3-db RF bandwidth of 40 kc (see Figure 4). This is known as the "zero-IF technique," which eliminates image problems since the image is used as part of the signal. A balanced mixer cancels out the local-oscillator signal and cross-modulation products in the output.

IF Filter

The IF filter determines the RF bandwidth of the radiometer. It consists of a low-pass

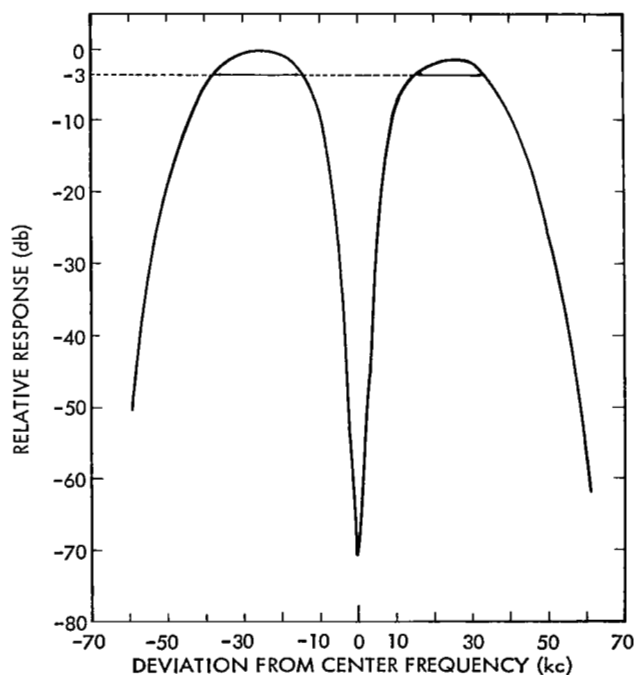


Figure 4—Effective RF bandwidth.

section with a 30-kc cutoff frequency followed by a high-pass section with a 10-kc cutoff frequency. Both sections are five element Butterworth filters. Figure 5 shows the pass band.

IF Amplifier

The IF amplifier is an RC-coupled audio amplifier providing about 90-db gain. AGC is provided by field-effect transistors AC-coupled across the emitter resistors of the first three stages. The transistors act as voltage-controlled resistors; and therefore they control the amount of emitter degeneration in the associated stages. Since maximum negative feedback occurs concurrently with maximum AGC control, the gain control is very smooth and distortion-free. This amplifier (Figure 6) produces about 90-db AGC.

Detectors

The IF output feeds into two detector stages (Figure 24).^{*} These detectors are basically similar in design, although one of them demodulates the 100-cycle modulation produced by the Dicke switch and the other senses the average level of the signal (and/or reference) and generates an AGC voltage. Each detector consists of an emitter-follower input amplifier driving a collector detector. This is simply a transistor amplifier operated in the square-law region of its characteristic. The collector circuits of these detectors also contain low-pass filters. The filter in the audio detector is adjusted to pass only the 100-cycle square wave modulation (Figures 7 and 8). In the AGC detector, this filter sets the AGC time constant to about 0.1 second. The outputs from these two detectors are then amplified by suitable single stage amplifiers.

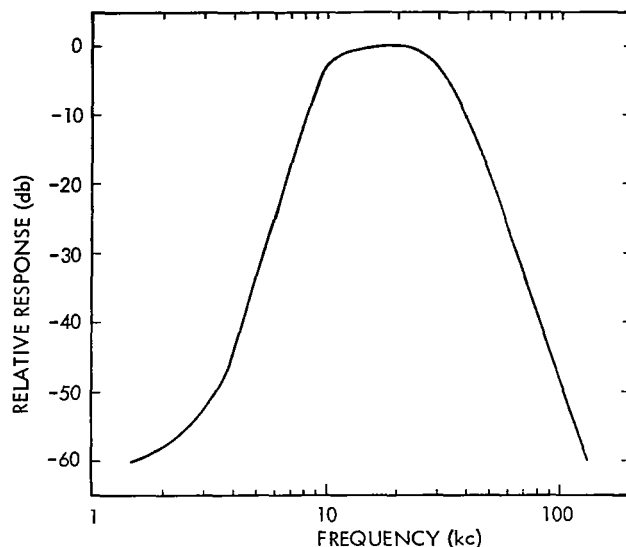


Figure 5—IF filter passband.

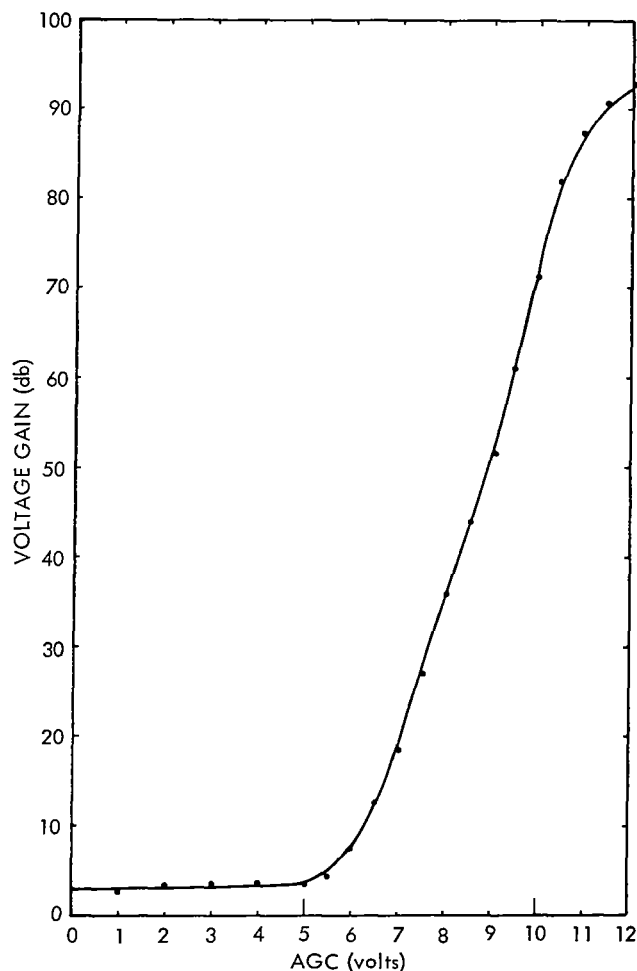
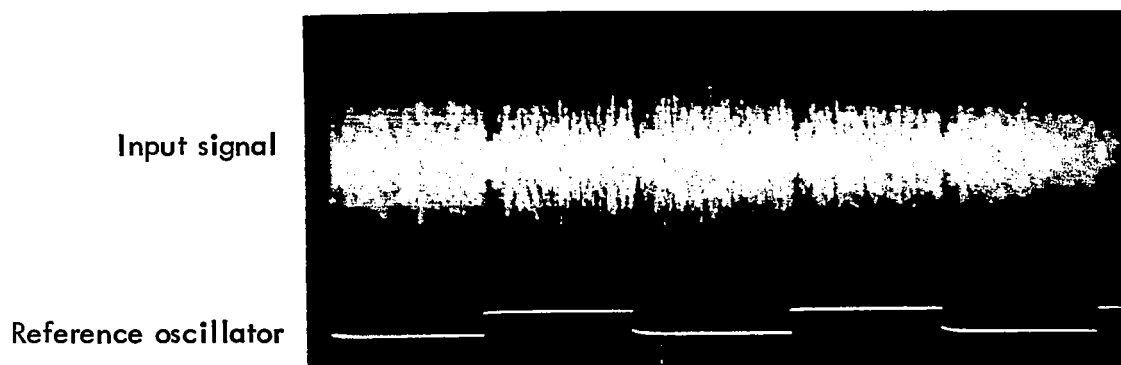


Figure 6—AGC characteristic of IF amplifier.

^{*}Figure is a fold-out schematic at end of this paper.



(a) Antenna noise $>$ noise source

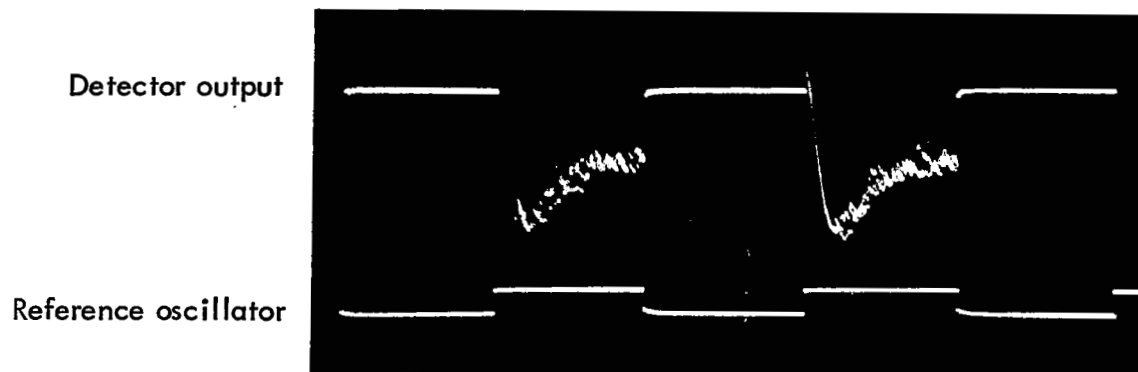


(b) Noise source = antenna signal

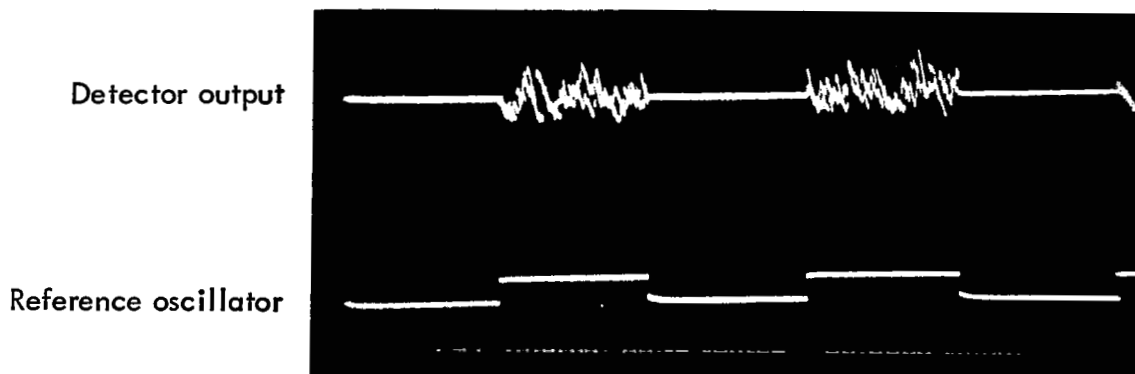


(c) Noise source $>$ antenna signal

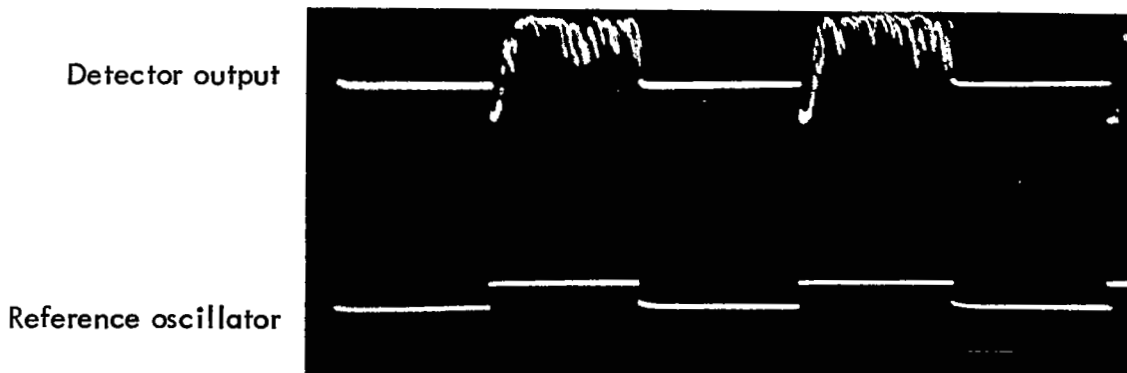
Figure 7—Detector input waveform.



(a) Internal noise source < antenna signal



(b) Internal noise source = antenna signal



(c) Internal noise source > antenna signal

Figure 8—Detector output waveform.

Phase-Sensitive Demodulator

The purpose of the phase-sensitive demodulator (Figure 24) is to detect the magnitude and phase of the Dicke-switch modulation on the signal input. The magnitude of this modulation is proportional to the comparison error between the input signal and the internal noise source. The demodulator therefore generates a dc error signal which is proportional to this error and whose sign (positive or negative) is determined by the phase of the modulation. This phase difference between the 100-cycle modulation and the reference square wave from the multivibrator can be either 0 or 180 degrees, depending on whether the antenna signal or the noise source has the larger magnitude.

The phase demodulator is actually a synchronous clamp to which the 100-cycle modulation is ac-coupled. Depending on which half-cycle of this 100-cycle square wave is clamped (phase of 0 or 180 degrees), either a positive or negative dc voltage is developed on the clamp side of the coupling capacitor.

Integrator

The error signal from the phase detector is routed into an operational amplifier connected as an integrator (Figure 24). This stage provides large dc gain and determines the time constant of the servo loop, which is set to about 0.1 second. This time constant was chosen to yield reasonably quick response to signal changes and still manage to smooth the 100-cycle pulses from the phase detector. The integrator dc output voltage controls the output level from the radiometer's noise source.

Noise Source

The noise source consists of a solid-state noise diode and a high-gain, wideband (0.2- to 10-Mc) amplifier with variable gain. It generates 10 mw of wideband noise at maximum output. This noise is measured by the thermistor bridge and then attenuated and fed into the radiometer front end.

The amplifier is a RC-coupled type with emitter followers between stages. This arrangement reduces the loading of the Miller-effect capacitances at the collectors of the common emitter stages and results in a broadband amplifier without the use of much feedback. Total amplifier gain is down 3 db at 200 kc and 10 Mc. The roll-off at high frequencies is due mainly to the output transformer and the gain-control arrangement used.

Low dc power consumption was an important requirement in designing the noise source; especially the output stage, which consumes more power than any other part of the radiometer. A transformer is used in the output because of this requirement, even though the bandwidth is slightly reduced. The output-stage power consumption is still high because, in order to obtain 10 mw of noise without clipping the peaks, the stage must be biased for a large peak-to-peak voltage swing. This is because the peak-to-RMS voltage ratio is greater for noise than for a sine wave.

The gain-control system chosen uses two field-effect transistors to vary the collector load impedance of two amplifier stages. A thermistor provides some temperature compensation. This system was selected because its control characteristics fitted well with the feedback-loop requirements, although it has slightly adverse effects on the amplifier bandwidth.

Range-Attenuator and Logic

The range attenuator (Figure 24) consists of some fixed pads along with three selectable attenuator sections of 0-db, 20-db, and 40-db attenuation. These sections are selected one at a time by diode switches.

The correct attenuator is chosen by measuring the noise-source control voltage with two Schmidt triggers. These sense when the noise source is out of range—one on the high side and the other on the low side. Whenever this occurs, the trigger starts a unijunction clock which steps a three-stage ring counter that drives the attenuator-section diode switches. The clock continues to step through the three available attenuations until the noise-source control voltage comes back in range.

Thermistor-Bridge

The real heart of radiometer precision is the thermistor-bridge power meter that samples the noise-source output. The bridge uses a feedback comparison technique similar to that used in the radiometer itself (see Figure 9), except that the noise-source output is compared with a dc reference.

The thermistor sensing element is (see Figure 24) connected to a bridge circuit involving an amplifier, a transformer, and a reference resistor. The feedback is such that with an unheated thermistor the bridge will oscillate. The oscillations heat the thermistor and lower its resistance until it closely matches the reference resistor. The oscillation then stabilizes and automatically adjusts with environmental temperature changes to maintain this equality.

Noise from the noise source is then fed through a Dicke switch to the thermistor. As the Dicke switch modulates the noise power at 10 cycles this modulation tries to cause fluctuation of the thermistor temperature, which in turn produces a modulation of the bridge excitation (see Figure 10). The thermistor resistance remains constant.

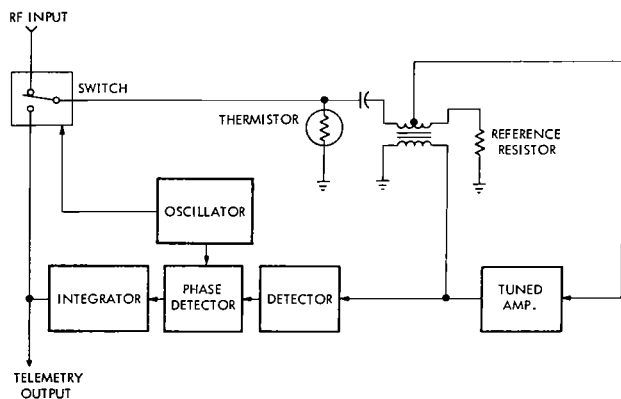
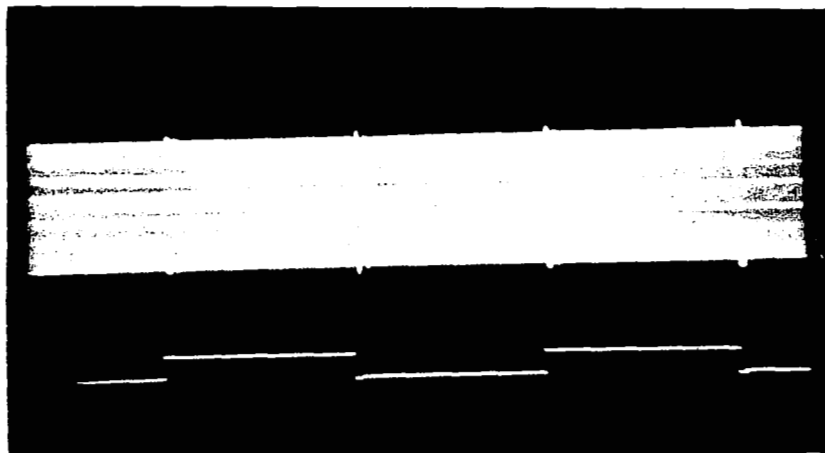


Figure 9—Thermistor bridge block diagram.

Thermistor excitation

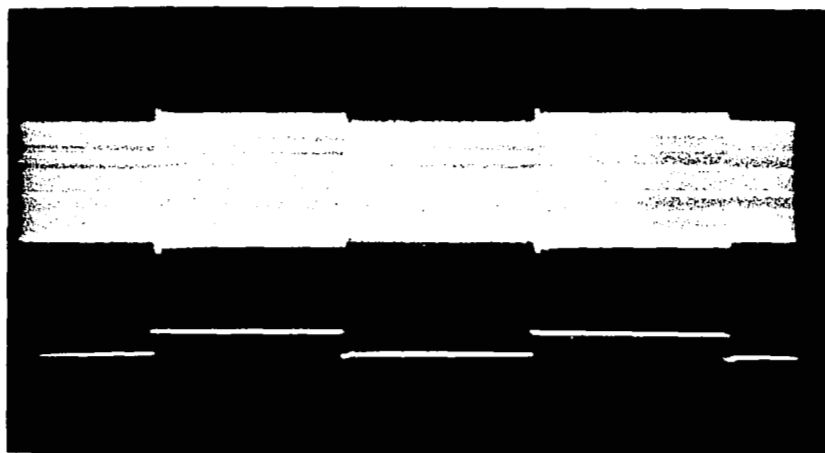
Reference square wave



(a) DC reference power = RF input power

Thermistor excitation

Reference square wave



(b) DC reference power \neq RF input power

Figure 10—Thermistor bridge common-mode oscillation.

The bridge-excitation modulation is synchronously detected and generates an error voltage, which causes the integrator to increase or decrease its output, V_0 , until the thermistor is heated equally by noise and dc. At this point:

$$\text{Noise Power} = \frac{V_0^2}{R_{\text{reference}}}$$

or conversely:

$$V_0 = \sqrt{P_{\text{noise}} R_{\text{ref.}}}$$

but since R is constant:

$$V_0 = k \sqrt{P_{\text{noise}}} .$$

This measurement is essentially independent of environmental conditions. The system time constant is about 0.5 second.

Reference Oscillator

The 100-cycle reference square wave could easily be generated by an ordinary multivibrator. (The multivibrator's two outputs automatically have the required 180-degree phase difference.) On the RAE spacecraft, however, there are three of these radiometers operating simultaneously. To preclude any mutual interference from the Dicke switches, the reference waveforms are all derived from the encoder clock (thus assuring synchronization between them). Only one of the two required square wave signals is routed from the encoder. The other out-of-phase signal is generated by a phase inverter (Figure 24) in each radiometer.

RESULTANT HARDWARE

The completed unit is shown in Figures 11 through 17. Chassis No. 1 contains the circuitry shown in Figure 23 and Chassis No. 2 contains the circuitry shown in Figure 24. The whole encapsulated unit weighs 3 lbs.; the total power drain is about 900 mw; size of the assembled unit is 7" x 7" x 3".

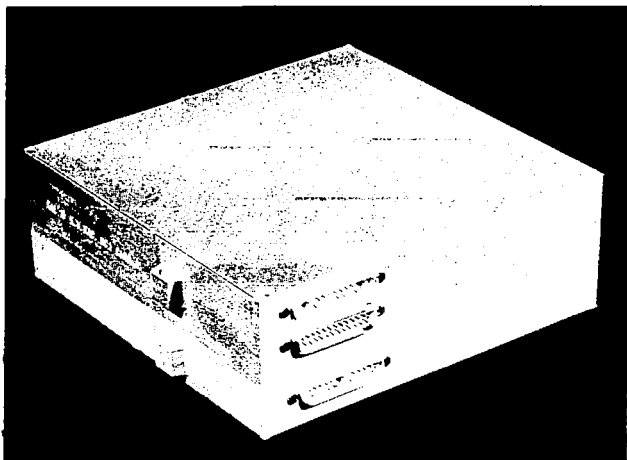


Figure 11—Assembled radiometer.

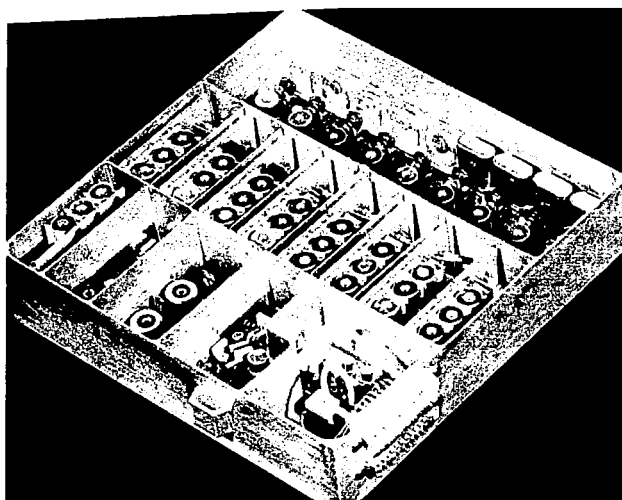


Figure 12—Radiometer Chassis No. 1, oblique view.

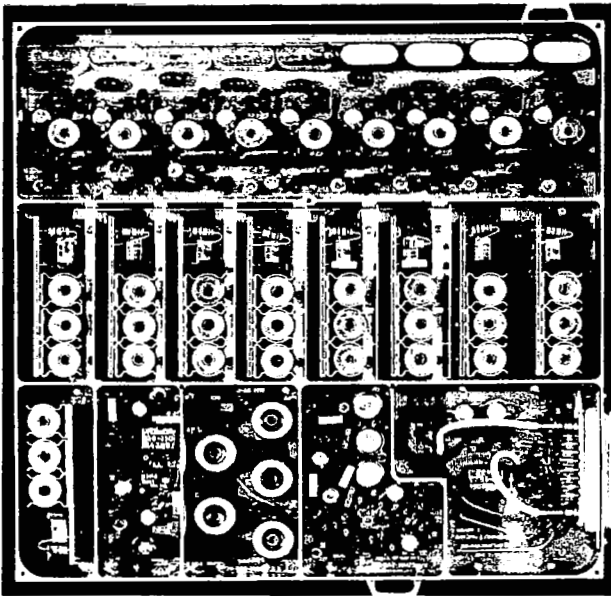


Figure 13—Radiometer Chassis No. 1, top view.

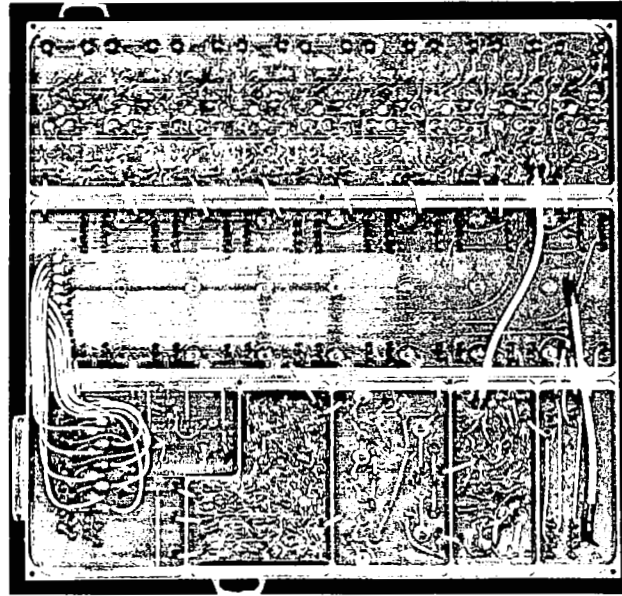


Figure 14—Radiometer Chassis No. 1, bottom view.

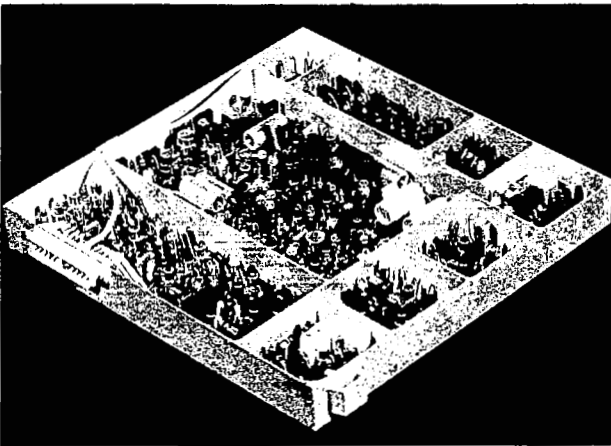


Figure 15—Radiometer Chassis No. 2, oblique view.

Figures 18 and 19 are calibration curves for the telemetry outputs. The "fine" output is the thermistor-bridge calibration curve. The "coarse" output is the noise-source calibration curve. Figures 20 and 21 show the effect of ambient temperature variations on portions of these curves. As expected, the fine output is considerably more stable than the coarse. Maximum temperature variation of the fine over an ambient temperature range of 80°C is about $\pm 1/2$ db. This is the same order of magnitude as the instantaneous peak noise on the output signals (determined

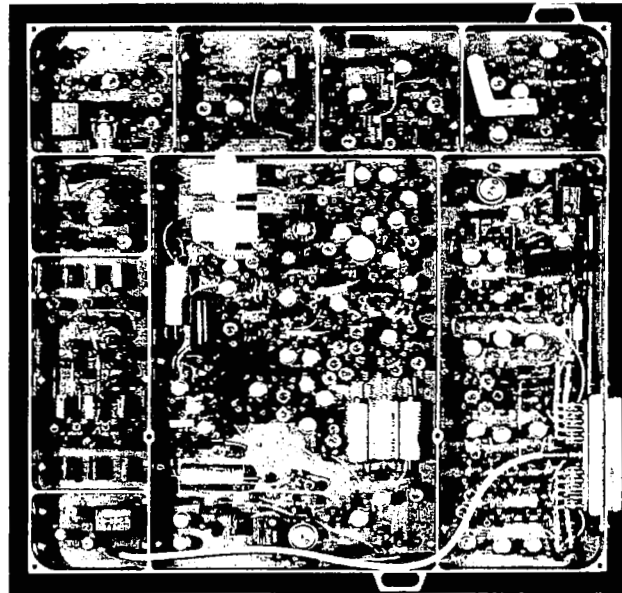


Figure 16—Radiometer Chassis No. 2, top view.



Figure 17—Radiometer Chassis No. 2, bottom view.

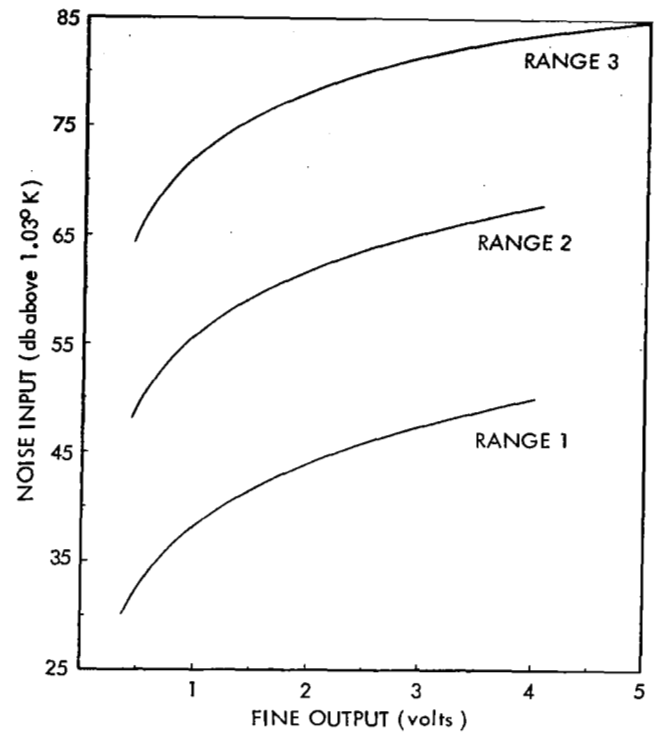


Figure 18—Typical fine output.

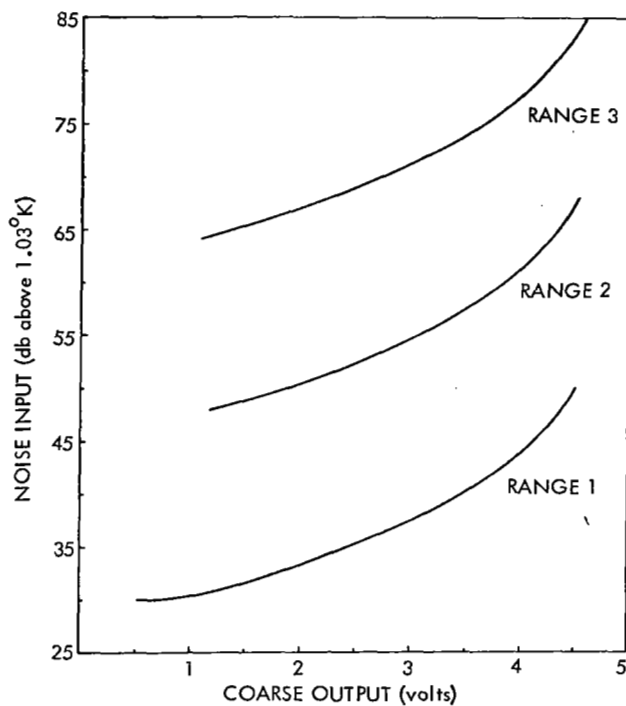


Figure 19—Typical coarse output.

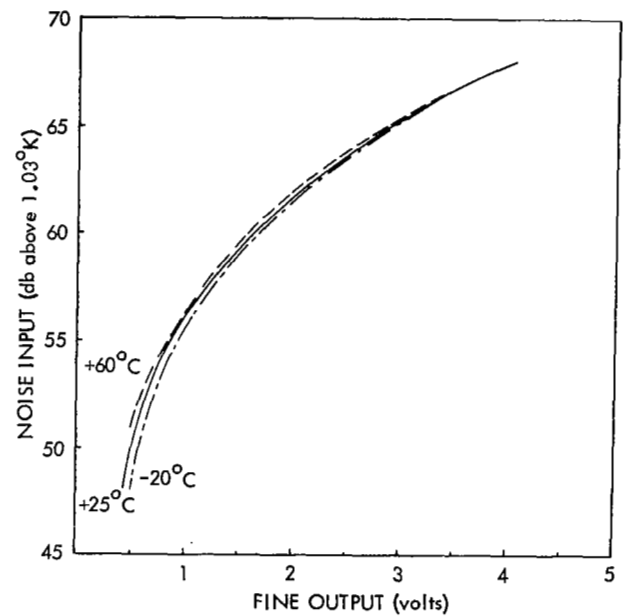


Figure 20—Typical fine output variation with temperature.

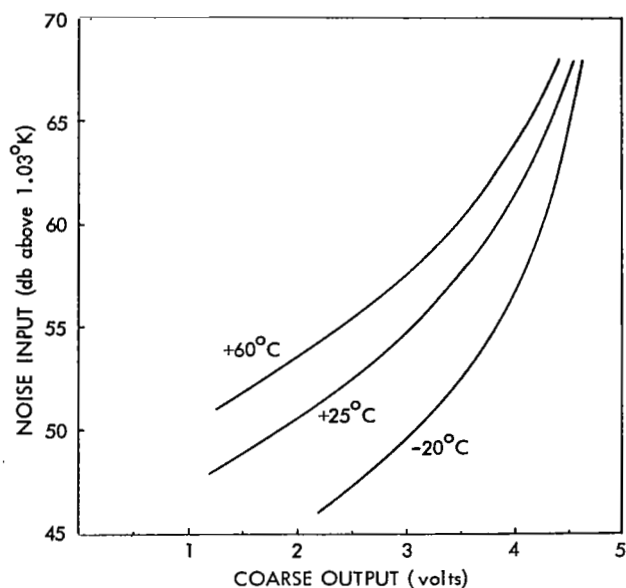


Figure 21—Typical coarse output variation with temperature.

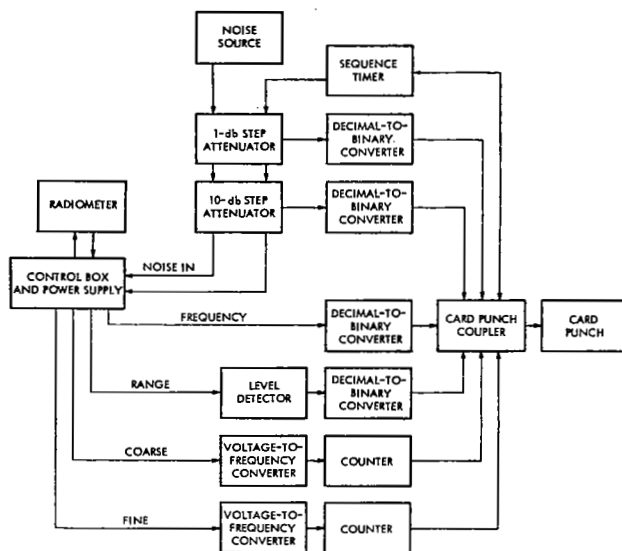


Figure 22—Automatic calibrator.

by the RF bandwidth and integration time constants). Power-supply voltage variations of ± 10 percent do not measurably affect calibration.

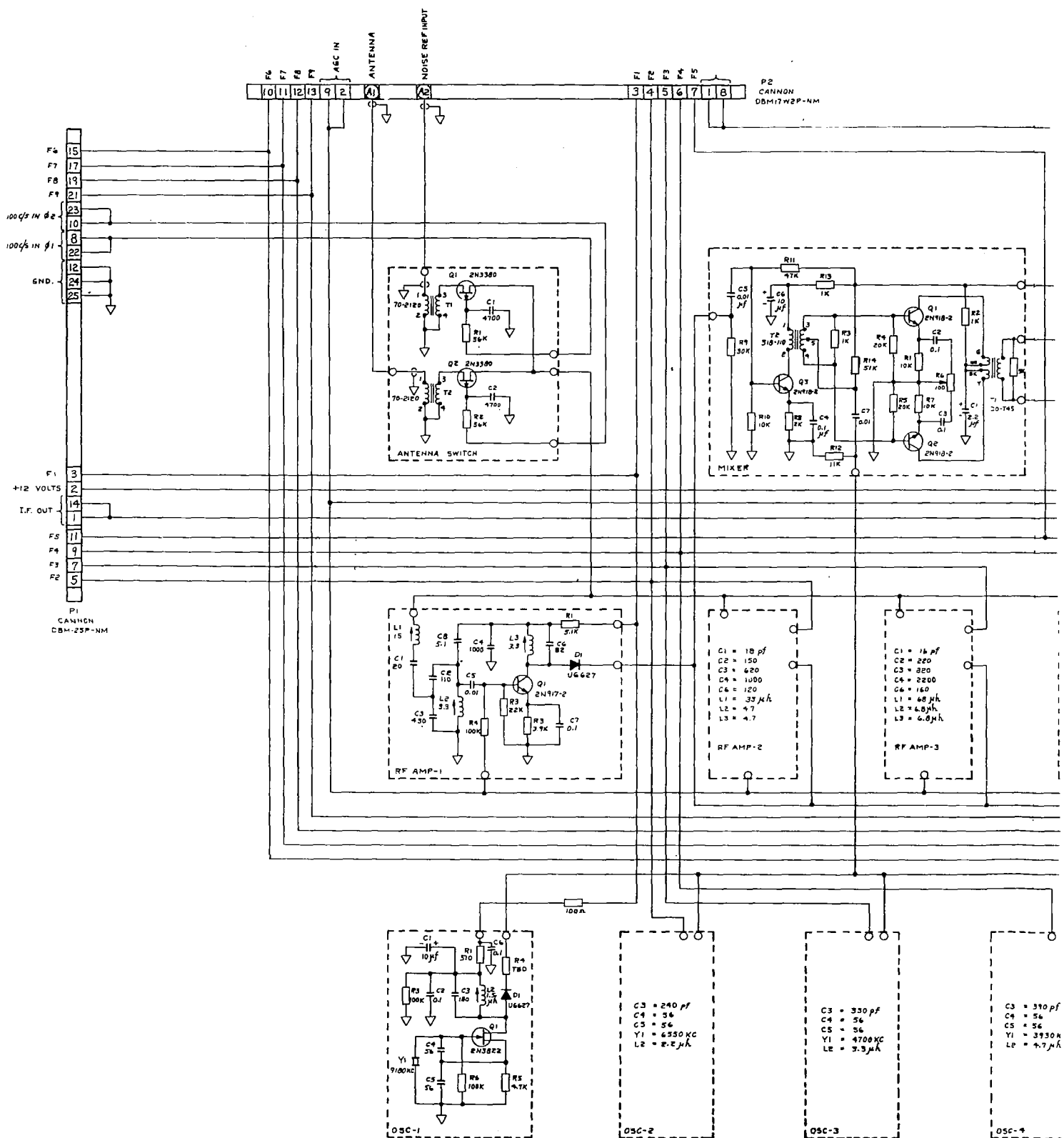
Since calibration of one of these radiometers over a 60-db input range for nine frequencies, three ambient temperatures, and both telemetry outputs involves over 3000 data points, it soon became evident that manual methods were inadequate. Therefore, an automatic calibrator was assembled (Figure 22); this puts the radiometer through its paces and punches the resulting data on IBM cards. These can be fed to a digital computer for curve plotting, synthesizing calibration equations, or organizing tables for data-reduction processing.

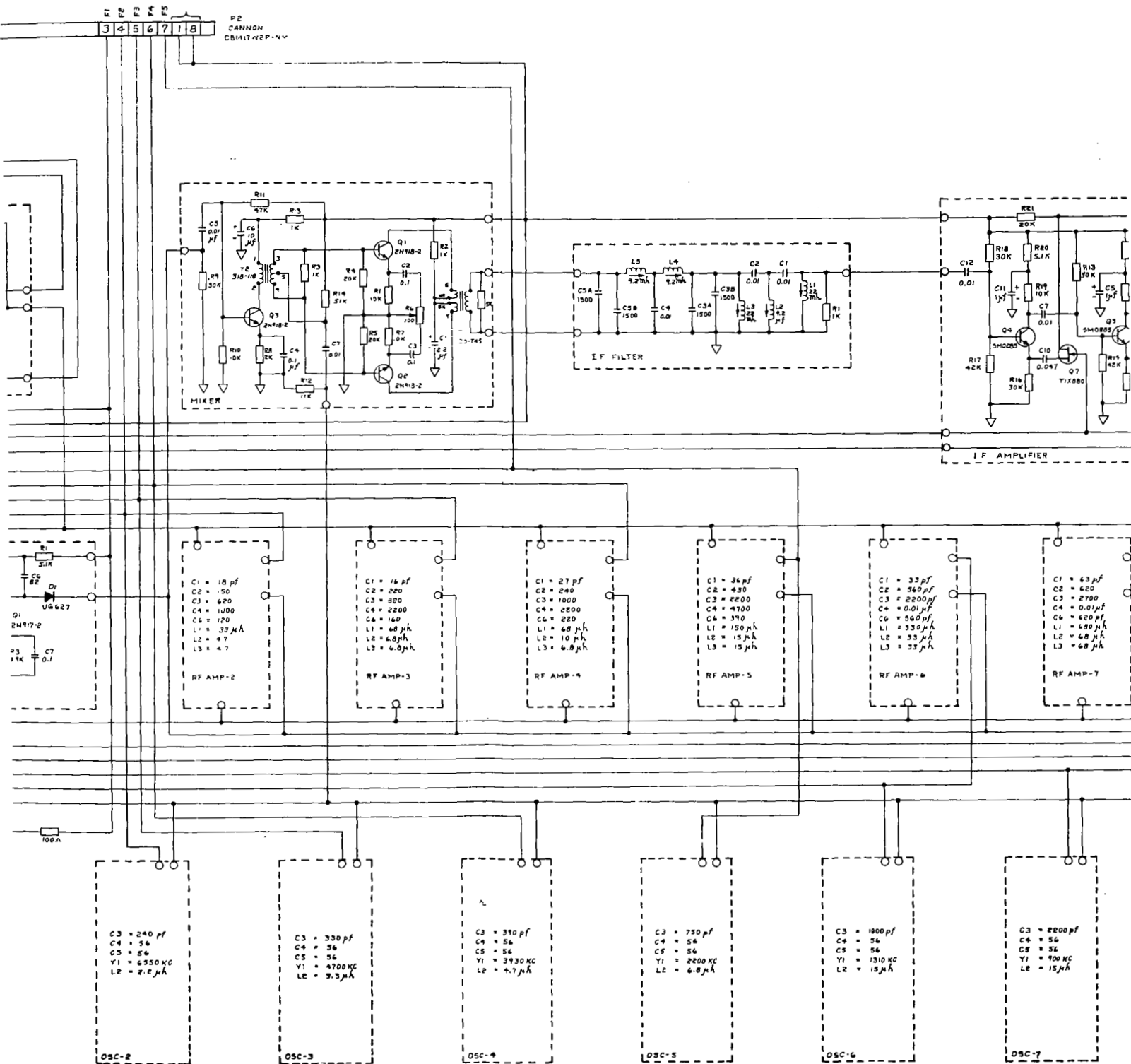
At the time of this writing, the RAE satellite has not been launched; however, some in-space experience has been accumulated. An early version of this radiometer was placed in orbit recently on board ATS-A; during the few months of operation it has lived up to all expectations.

Goddard Space Flight Center
National Aeronautics and Space Administration
Greenbelt, Maryland, October 18, 1967
697-01-01-01-51

REFERENCES

1. Machin, K. E., Ryle, M., and Vonberg, D.D., "The Design of an Equipment for Measuring Small Radio-Frequency Noise Powers," *Proc. IEE*, 99: III, 127-134, May 1952.
2. Strum, P. D., "Considerations in High Sensitivity Microwave Radiometry," *Proc. IRE*, 46: 43-53, Jan. 1958.





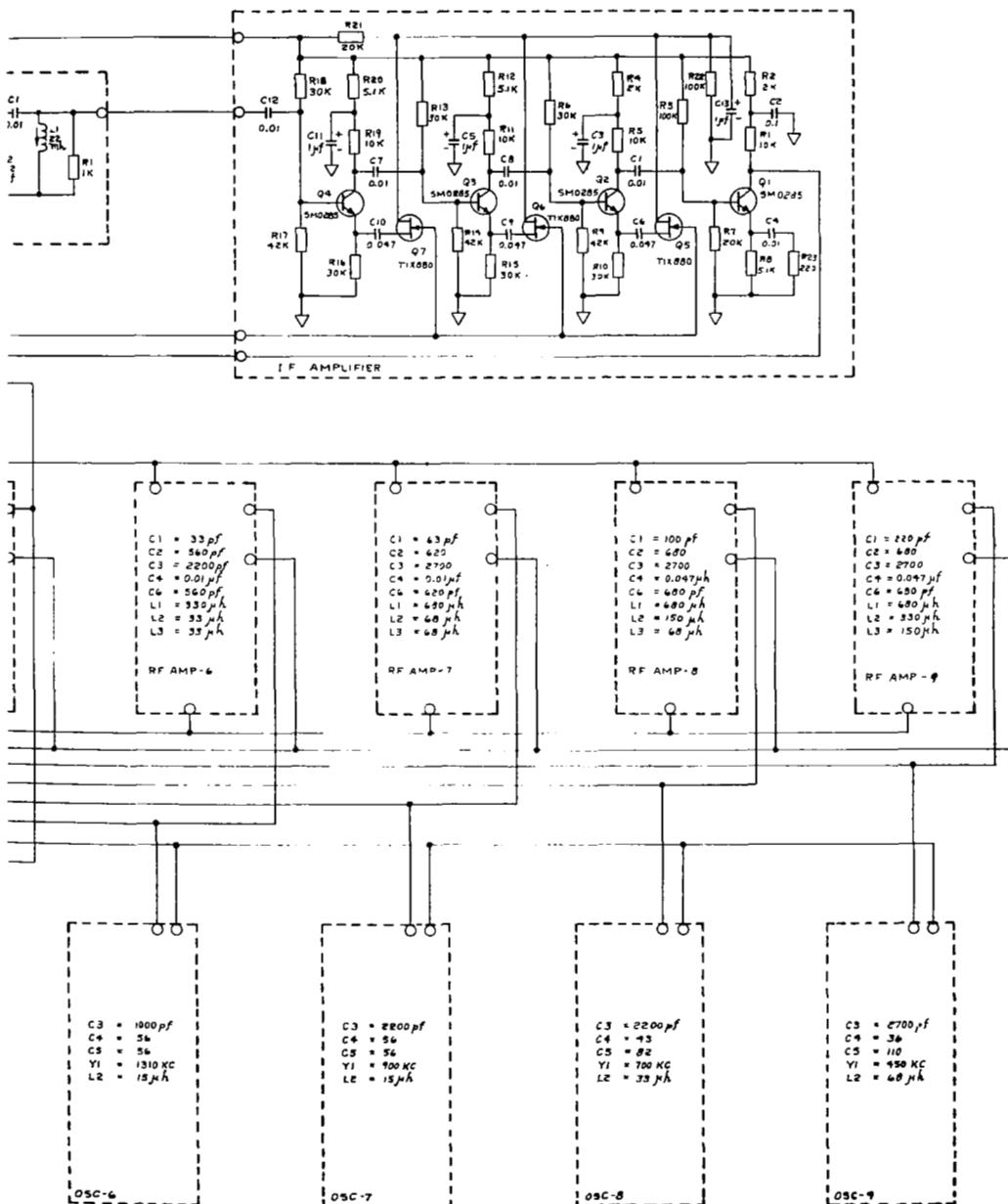
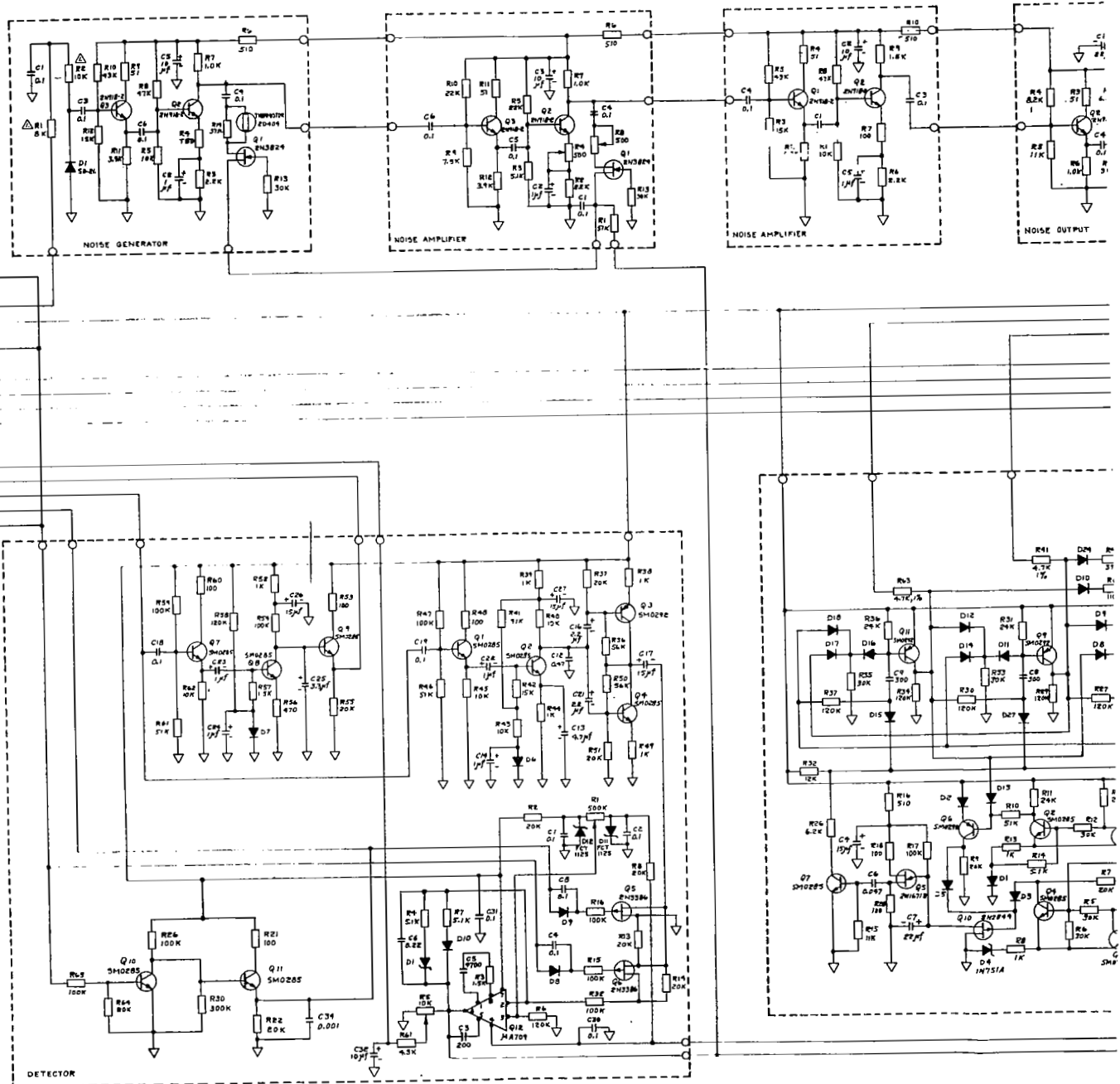
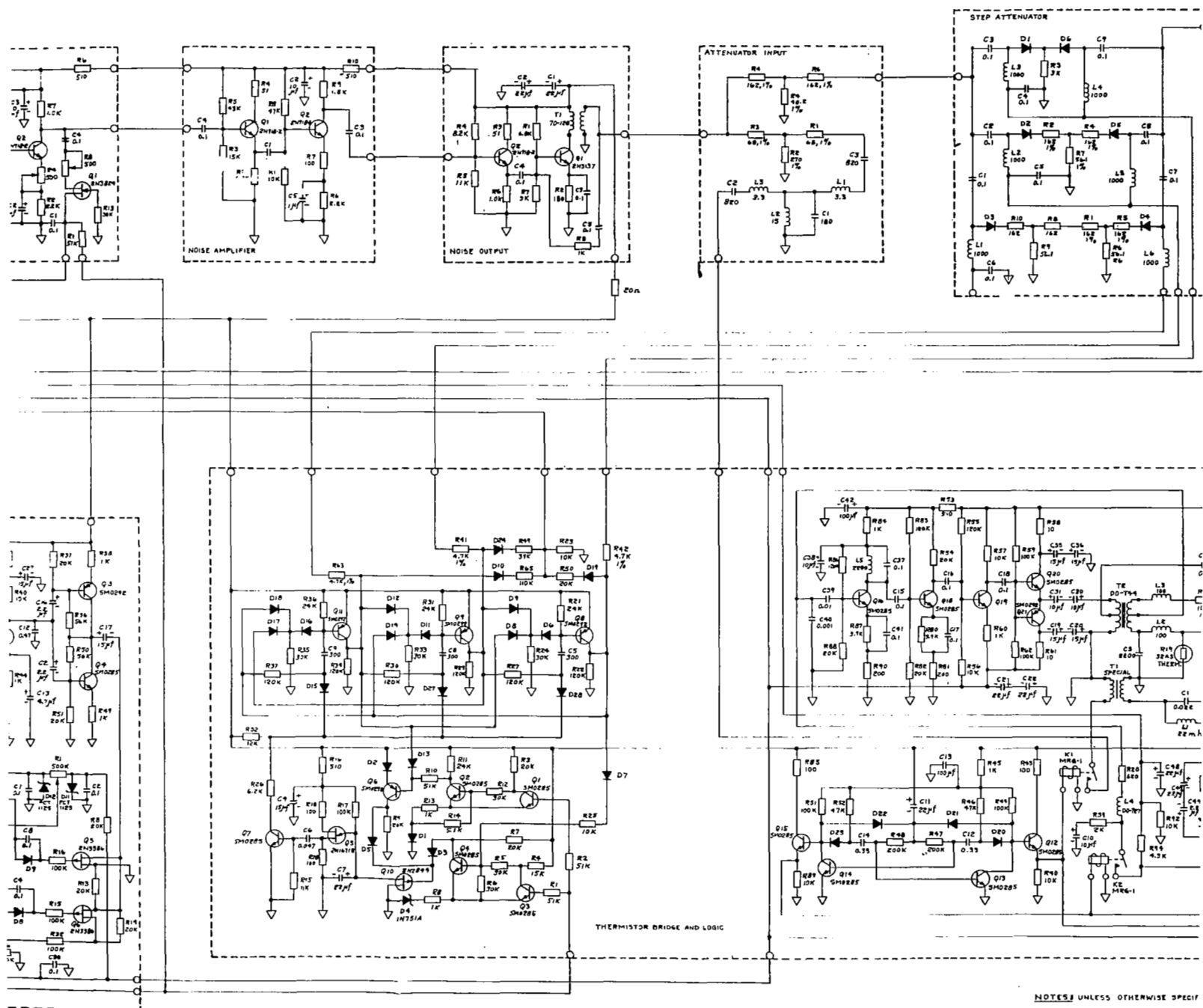


Figure 23-Schematic diagram-RAE Chassis No. 1.





NOTES: UNLESS OTHERWISE SPECIFIED
 1. TYPICAL - MUST BE MATCHED TO
 2. CAPACITOR VALUES ≥ 1 ARE IN μ F
 3. CAPACITOR VALUES < 1 ARE IN pF
 4. INDUCTOR VALUES ARE IN μ H
 5. ALL DIODES ARE UG-4007

Figure 24



FIRST CLASS MAIL

010 001 34 01 345 64154 00001
AIR FORCE WEAPONS LABORATORY/SL/7
KIRTLAND AIR FORCE BASE, NEW MEXICO 87117

ALL INFORMATION CONTAINED HEREIN IS UNCLASSIFIED
DATE 7/11/07 BY 60322 UCBAW

POSTMASTER: If Undeliverable (Section 158
Postal Manual) Do Not Return

"The aeronautical and space activities of the United States shall be conducted so as to contribute . . . to the expansion of human knowledge of phenomena in the atmosphere and space. The Administration shall provide for the widest practicable and appropriate dissemination of information concerning its activities and the results thereof."

—NATIONAL AERONAUTICS AND SPACE ACT OF 1958

NASA SCIENTIFIC AND TECHNICAL PUBLICATIONS

TECHNICAL REPORTS: Scientific and technical information considered important, complete, and a lasting contribution to existing knowledge.

TECHNICAL NOTES: Information less broad in scope but nevertheless of importance as a contribution to existing knowledge.

TECHNICAL MEMORANDUMS: Information receiving limited distribution because of preliminary data, security classification, or other reasons.

CONTRACTOR REPORTS: Scientific and technical information generated under a NASA contract or grant and considered an important contribution to existing knowledge.

TECHNICAL TRANSLATIONS: Information published in a foreign language considered to merit NASA distribution in English.

SPECIAL PUBLICATIONS: Information derived from or of value to NASA activities. Publications include conference proceedings, monographs, data compilations, handbooks, sourcebooks, and special bibliographies.

TECHNOLOGY UTILIZATION PUBLICATIONS: Information on technology used by NASA that may be of particular interest in commercial and other non-aerospace applications. Publications include Tech Briefs, Technology Utilization Reports and Notes, and Technology Surveys.

Details on the availability of these publications may be obtained from:

SCIENTIFIC AND TECHNICAL INFORMATION DIVISION
NATIONAL AERONAUTICS AND SPACE ADMINISTRATION
Washington, D.C. 20546